(27) Rudin, A. "Elements of Polymer Science and Engineering"; Academic Press: New York, 1982; Chapter 11.
(28) Grapengeter, H. H.; Kosfeld, R.; Offergeld, H. W. *Polymer* **1980**, *21*, 829.
(29) Zeman, A.; Patterson, D. *Macromolecules* **1972**, *5*, 513.
(30) van Geet, A. L. *Anal. Chem.* **1970**, *42*, 679.
(31) Opella, S. J.; Nelson, D. J.; Jardetzky, O. J. *J. Chem. Phys.* **1976**, *64*, 2533.

Poly(1,4-*trans*-cyclohexanediyldimethylene succinate): A Structural Determination Using X-ray and Electron Diffraction

François Brisse* and Bruno Rémillard

Département de Chimie, Université de Montréal, C.P. 6210, Succ. A, Montréal, Québec, H3C 3V1 Canada

Henri Chanzy

Centre de Recherche sur les Macromolécules Végétales (CNRS), B.P. 68, 38042-St. Martin d'Hères, France.† *Received October 3, 1983*

ABSTRACT: Poly(1,4-*trans*-cyclohexanediyldimethylene succinate) or poly(*t*-CDS) has a monoclinic unit cell of dimensions $a = 6.486$ Å, $b = 9.482$ Å, $c = 13.51$ Å, and $\beta = 45.9°$ and belongs to the space group $P2_1/n$. The calculated crystalline density of 1.259 g cm^{-3} indicates that there is one chemical unit per fiber repeat and two chains per unit cell. Micro single crystals of poly(*t*-CDS) were obtained by recrystallization from toluene. The crystals are lamellar, 100 Å thick, and diamond-shaped with typical spiral growths. Electron diffraction intensities were recorded for three distinct orientations of the micro single crystals of poly(*t*-CDS) using an electron microscope equipped with a tilting stage. The geometry of the chemical repeat unit was derived from the crystal structure of 1,4-*trans*-cyclohexanedimethylene 3,3′-bis(methoxycarbonyl)dipropionate, a model compound for this polymer. The structure was established by conformational and packing analyses and confirmed by X-ray and electron intensity calculations. The value of the conventional R_w factor is 0.206 for 29 observed diffraction spots. With the electron diffraction data, $R_w = 0.199$ for 87 observed reflections. The chain conformation and the packing of the chains in the unit cell are discussed and compared with the crystal structures of other aliphatic polyesters. The —O—CH_2—(C_6H_{10})—CH_2—O— "flexible" segment of the polyester has the conformation $t_g^t(t\pm gt)_t^{-g}t$ (g, gauche; t, trans) while the succinate group is in the trans conformation.

Introduction

The first studies on aliphatic polyesters were reported in the late 1930s by Fuller and Erickson[1] or a series of ethylene glycol polyesters and by Fuller, Frosch, and Pape[2] for a series of trimethylene glycol polyesters. Only qualitative conclusions concerning the crystalline conformations of the polymers were drawn. The first crystalline structures were established in the ethylene glycol polyesters series, $\{O(CH_2)_2OCO(CH_2)_xCO\}_n$, where $x = 0$, 2, 4, and 6. Ueda, Chatani, and Tadokoro[3] studied the crystalline structure of poly(ethylene oxalate) (PE0) and poly(ethylene succinate) (PE2) ($x = 0$ and 2, respectively) and Turner-Jones and Bunn[4] determined the crystal structure of poly(ethylene adipate) (PE4) and poly(ethylene suberate) (PE6) ($x = 4$ and 6, respectively). In each case, the glycol portion shows a considerable deviation from the fully planar conformation, while the acid portion is in the fully extended conformation, except for PE2.

The crystal structure of poly(1,4-*trans*-cyclohexanediyldimethylene terephthalate) or poly(*t*-CDT) has recently been reported.[5] Since it has been observed that a succinate and a terephthalate group are often interchangeable, we have undertaken to determine the crystal structure of poly(1,4-*trans*-cyclohexanediyldimethylene succinate) or poly(*t*-CDS), $\{OCH_2(C_6H_{10})CH_2OCO(CH_2)_xCO\}_n$, where $x = 2$.

Electron diffraction patterns of polymer single crystals have often been obtained but were rarely used for the elucidation or the confirmation of the polymer structure. In this case, good-quality micro single crystals of poly(*t*-CDS) were grown and their electron diffractograms were recorded in an electron microscope fitted with a tilting stage. The three-dimensional intensity data have been used to confirm the proposed structure of poly(*t*-CDS).

Experimental Section

Sample Preparation. Poly(*t*-CDS) powder was obtained from Aldrich Chemical Co., Inc. The molecular weight of the polyester, calculated from tonometric analysis,[6] is equal to 4200. At this low molecular weight, the polyester is highly crystalline but could not be drawn. Therefore, the polymer was treated with tolylene 2,4-diisocyanate to produce a higher molecular weight compound, using the method described by Iwakura, Taneda, and Uchida.[7] After treatment, the molecular weight was increased to 6900. A similar approach has been used by Ueda et al.[3] and Turner-Jones and Bunn[4] and for PE2 and PE4, respectively. This treatment does not affect the structural determination since it is believed that only the pure ester sections of the chains crystallize while the amide portions remain in the amorphous region of the polymer. Fibers of poly(*t*-CDS) were then obtained by quick quenching of the molten polymer in a mixture of dry ice/methanol followed by cold drawing. The fibers were annealed under tension at 90 °C for about 30 min. Micro single crystals of poly(*t*-CDS) suitable for electron diffraction could be grown in the following manner: a solution of 0.5% of commercial poly(*t*-CDS) in toluene was prepared at 80 °C. The solution was cooled slowly to 48 °C, where a slight precipitation was observed. The solution was kept 12 h at this temperature. The polymer was redissolved and the solution was brought down to 55 °C. Cooling the 55 °C solution at a rate of 1 °C/12 h brought about reprecipitation at 51 °C. This temperature was maintained for 48 h. Room temperature was reached

† Affiliated with the Scientific and Medical University of Grenoble.

0024-9297/84/2217-1980$01.50/0

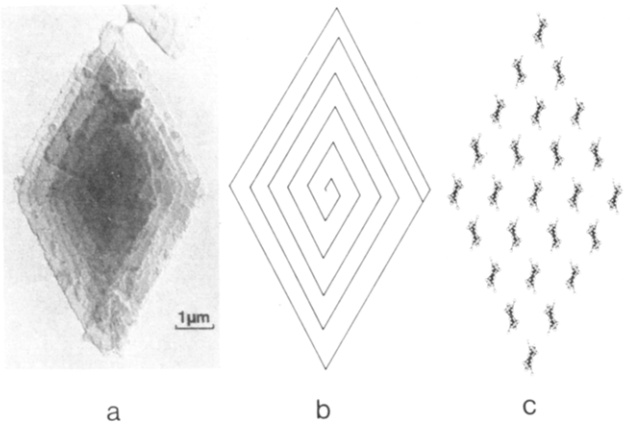

Figure 1. (a) Typical micro single crystal of poly(*t*-CDS). (b) Spiral terraced structure of the crystal. (c) Disposition of the chains in relation to the outline of the crystal shape.

at the rate of approximately 0.25 °C/h.

X-ray and Electron Diffraction. X-ray fiber diagrams were recorded in Warhus, precession or Weissenberg, cameras using the multiple-film technique and nickel-filtered Cu Kα radiation. Some diffracted intensities were visually estimated while others were measured with a Joyce-Loebl microdensitometer. The structure factors were then derived after correction for the relevant Lorentz and polarization factors.

For electron microscopy and diffraction, drops of a suspension of poly(*t*-CDS) single crystals in toluene were evaporated on carbon grids. In order to evaluate the thickness of the crystals, an aqueous suspension of small latex spheres, 0.109 μm in diameter, was deposited on the grids, which were then shadowed by tungsten/tantalum at an angle of 30°. For *d*-spacing calibration of the electron diffractograms, gold was evaporated on some of the grids. Micrographs and electron diffraction patterns were recorded on photographic film using a Philips EM400T electron microscope equipped with a tilting stage. The electron microscope was used at 80 kV for imaging and at 120 kV in the diffraction mode. The intensities of the electron diffractograms were visually estimated with the use of a calibrated intensity scale.

Model Compound. One of the model compounds related to poly(*t*-CDS) is 1,4-*trans*-cyclohexanedimethylene 3,3′-bis(methoxycarbonyl)dipropionate. This compound was synthesized and its crystal structure established[8] from three-dimensional X-ray diffraction data for the sole purpose of this work. The geometrical data found for this molecule were used in the chain description of poly(*t*-CDS) necessary in the conformational and packing analyses.

An intrinsic torsional potential with a threefold barrier of 2.8 kcal mol^{-1} was assigned to rotations about the bonds while the torsional barrier for the C–O bond was taken to be zero. Rotation about the carboxyl group was not allowed. The van der Waals interactions between nonbonded atoms were evaluated with 6–12 potential functions, with the parameters proposed by Scott and Scheraga.[9,10] Electrostatic interactions were evaluated by assigning partial charges to the atoms using a Coulomb's law potential function.[11] The following values for the bond moments[12] were used: C–C = 0.0, C–O = 0.82, C⋯O = 0.74, C=O = 2.34, and C–H = 0.38 D. Isoenergy contours were plotted at 1 kcal mol^{-1} intervals with respect to the minimum energy, which was arbitrarily set at zero.

Structure Determination

Crystal Morphology. A typical micro single crystal in the shape of a diamond is shown in Figure 1a. The crystal dimensions are 5–8 μm for the shortest diagonal and 8–12 μm for the longest diagonal. Each lamella of a crystal has a thickness of about 100 Å. The diamond-shaped crystals show that characteristic spiral terraced structure resulting from a screw dislocation growth (Figure 1b).

Unit Cell Dimensions and Space Group. The X-ray powder diagrams of all the poly(*t*-CDS) preparations are the same, confirming the integrity of the polyester after various treatments. Electron diffractograms recorded for three different tilt angles are shown in Figure 2a. The tilt axis was made to coincide with the longest diagonal of the single crystal. With the gold rings as calibration standard, a_0(Au) = 4.07825 Å[13], the *d* value of each diffraction spot was evaluated and averaged from a total of ten different diffraction films. The indexing of the electron diffraction patterns first yielded a monoclinic unit cell of dimensions a = 6.291 Å, b = 9.217 Å, c = 9.794 Å, and β = 106.3°. The powder diffraction pattern of the polyester could also be indexed with this unit cell. However, since the X-ray fiber diagram (Figure 3a) reveals a fiber repeat of the order of 13.5 Å, the above unit cell was transformed into the one given in Table I. This new unit cell is compatible with both the X-ray and electron diffraction patterns. The three electron diffraction patterns which have the b^* axis in common (the tilt axis) are shown indexed in Figure 2b. On Figure 2c, which shows the a^*c^* projection, (i.e., b^* perpendicular to the plane of the figure), the orientation of each of the three electron diffractograms is materialized by their traces on the a^*c^* plane. Altogether 87 individual electron diffraction reflections to a resolution of 1.01 Å were observed. The 29 diffraction spots of the fiber diagram, up to the sixth layer line, to a resolution of 1.62 Å, have also been indexed (Figure 3b). The monoclinic unit cell dimensions, obtained by a least-squares refinement of the combined X-ray and electron diffraction data, and other crystallographic data of interest are presented in Table I. The indexed list of the observed and calculated $\sin^2\theta$ is given in Table II. The observed systematic absences, for $0k0$, $k \neq 2n$ and $h0l$, $h + l \neq 2n$, are characteristic of the centrosymmetric space group $P2_1/n$. The comparison of the calculated density with the one measured in a $ZnCl_2$ solution indicates that there are two polymeric chains per unit cell. Since in $P2_1/n$ the general position is of order 4, the two chains must occupy special positions in the unit cell. One of them is along *c* while the second one, parallel to *c*, passes through the center of the *ab* plane. Furthermore, the center of the cyclohexyl groups as well as the midpoint of the CH_2–CH_2 bond in the succinate part must coincide with the centers of symmetry of the unit cell.

Table I
Crystal Data for Poly(*t*-CDS)

$[C_{12}H_{18}O_4]_n$	β = 45.9 (5)°
mol wt = 226.28	V = 597 Å^3
monoclinic	
space group $P2_1/n$	Z = 2
a = 6.486 (10) Å	d_{obsd} = 1.23 g cm^{-3}
b = 9.482 (10) Å	d_{calcd} = 1.259 g cm^{-3}
c = 13.51 (5) Å[a]	λ(Cu K$\bar{\alpha}$) = 1.54178 Å

[a] Fiber repeat.

Determination of the Chain Conformation. Figure 4 presents side by side the polymer and its model compounds, while in Figure 5, the bond distances and angles derived from the structure of the model compound[8] are given. The 1,4-*trans*-cyclohexanedimethanol moiety and succinate group lie on crystallographic centers of symmetry. The following torsion angles define the chain conformation (Figure 6): ϕ_1 = C(2)–C(4)–O(2)–C(5) = $-\phi_1'$, ϕ_2 = C(1)–C(2)–C(4)–O(2) = $-\phi_2'$, ϕ_3 = C(4)–C(2)–C(1)–C(3′) = $-\phi_3'$, ϕ_4 = C(4)–C(2)–C(3)–C(1′) = $-\phi_4'$, ϕ_5 = C(2)–C(1)–C(3′)–C(2′) = $-\phi_5'$.

Since the succinate group is on a center of symmetry, C(5)–C(6)–C(6′)–C(5′) = 180°. Furthermore, the cyclohexanediyl conformational angles defined by ϕ_3, ϕ_4, ϕ_5 and their centrosymmetrically related counterparts do not need to be varied and the following fixed values obtained from

Table II
Comparison of the Observed and Calculated $\sin^2\theta$ Obtained from the Fiber Diagram and the Electron Diffractograms of Poly(t-CDS)

	$\sin^2\theta$			$\sin^2\theta$	
hkl	obsd	calcd	hkl	obsd	calcd
		Fiber Diagram			
020	0.0260	0.0264	133	0.0882	0.0886
110	0.0341	0.0337	204	0.0630	0.0641
120	0.0539	0.0533	214	0.0714	0.0705
140	0.1333	0.1321	254	0.2277	0.2284
220		0.1350	344		0.2320
230	0.1685	0.1676	105	0.0936	0.0935
111	0.0215	0.0218	115	0.1043	0.1002
021	0.0324	0.0328	225		0.1105
11$\bar{1}$	0.0588	0.0582	125	0.1211	0.1201
12$\bar{1}$	0.0785	0.0778	235	0.1436	0.1434
041	0.1129	0.1121	145	0.1895	0.1895
241	0.1838	0.1834	216	0.1244	0.1236
112	0.0221	0.0225	316	0.1493	0.1505
122	0.0426	0.0423	116		0.1513
103	0.0299	0.0293	326	0.1665	0.1701
123	0.0552	0.0556	126		0.1713
013	0.0641	0.0635			
		Electron Diffractogram A, $nk0$ Reflections			
020	0.0266	0.0264	200	0.1086	0.1093
040	0.1039	0.1056	210	0.1152	0.1156
060	0.2320	0.2376	230	0.1658	0.1676
080	0.4218	0.4223	240	0.2127	0.2134
110	0.0340	0.0337	250	0.2707	0.2724
120	0.0543	0.0533	310	0.2491	0.2520
130	0.0850	0.0861	320	0.2695	0.2712
140	0.1316	0.1321	330	0.2997	0.3037
150	0.1894	0.1913	340	0.3468	0.3493
		Electron Diffractogram B, nkn Reflections			
101	0.0163	0.0154	303	0.1376	0.1384
111	0.0232	0.0218	313	0.1444	0.1446
121	0.0426	0.0415	323	0.1639	0.1640
131	0.0750	0.0744	333	0.1960	0.1966
141	0.1204	0.1204	343	0.2413	0.2424
151	0.1787	0.1787	353	0.2998	0.3014
161	0.2473	0.2522	414	0.2502	0.2521
181	0.4320	0.4367	434	0.3024	0.3038
202	0.0614	0.0615	444	0.3474	0.3495
212	0.0683	0.0678	454	0.4060	0.4084
222	0.0879	0.0874	464	0.4741	0.4804
232	0.1202	0.1201	505	0.3805	0.3844
242	0.1653	0.1660	525	0.4067	0.4095
262	0.2923	0.2975	555	0.5425	0.5461
272	0.3798	0.3830			
		Electron Diffractogram C, $n,k,2n$ Reflections			
112	0.0209	0.0225	234	0.1213	0.1230
122	0.0426	0.0423	244	0.1665	0.1691
132	0.0745	0.0752	254	0.2279	0.2284
142	0.1195	0.1213	264	0.2976	0.3008
152	0.1810	0.1807	316	0.1467	0.1505
162	0.2508	0.2532	326	0.1755	0.1701
182	0.4371	0.4378	336	0.2009	0.2029
204	0.0624	0.0641	346	0.2457	0.2489
214	0.0693	0.0705	356	0.3077	0.3081
224	0.0895	0.0902			

the model compound are used: $\phi_3 = -178.7$, $\phi_4 = 179.0$, and $\phi_5 = 56.8°$. Therefore, only a (ϕ_1,ϕ_2) energy map needs to be computed. This map is shown in Figure 6. The (ϕ_1,ϕ_2) pairs for the calculated minima are compared in Table III with the actual conformation of the model compound. Only two energetically favored conformations match the fiber repeat and are close to that of the model compound. In each case, $\phi_1 = 180°$, while $\phi_2 = 69$ or $-171°$. These two conformations are equivalent according to which side of cyclohexanediyl group is used.

Table III
Conformational Analysis of Poly(t-CDS)

Conformation Angles for the Energy Minima E		
ϕ_1, deg	ϕ_2, deg	E, kcal mol^{-1}
75	−171	0.00
−75	−51	0.12
−95	69	0.28
95	69	0.52
−100	−171	0.62
100	−51	0.87
180	−171	1.06
175	−51	1.22
180	69	1.25
Conformation in the Model Compound		
−169.8	−173.4	
	64.7	
Conformation Adopted for Poly(t-CDS)		
−179.0	−171.2	
	64.7	

Table IV
Fractional Atomic Coordinates[a] for Poly(t-CDS)

atom	x	y	z
O(1)	288	−2005	3757
O(2)	−445	−231	2946
C(1)	1665	576	263
C(2)	−785	−419	1282
C(3)	−1212	−1412	541
C(4)	−386	−1230	2108
C(5)	−75	−772	3727
C(6)	−272	313	4584
H(11)	351	4	−39
H(12)	192	124	75
H(21)	−264	11	192
H(31)	−289	−205	122
H(32)	49	−205	−10
H(41)	−196	−194	271
H(42)	149	−174	147
H(61)	112	109	599
H(62)	−220	77	521

[a] $\times 10^4$ for C and O atoms, $\times 10^3$ for H atoms.

Packing Analysis. The relative orientation of the chains in the unit cell remains to be found. As the chains must pass through the symmetry centers of the unit cell, the rotation around the c axis is the only packing parameter. The interchain interactions are minimized following William's procedure.[14] The packing index $R_p = \sum w(d_0 - d_{ij})^2$, measures the degree of interactions between adjacent chains, where d_0 is a reference distance, d_{ij} the distance between atoms i and j of two adjacent chains, and w a weighting parameter. The values of d_0 and w used here are taken from William.[14] The packing index gives an indication of how weak these interactions are. The plot of R_p as a function of the chain orientation is reported in Figure 7. An R_p minimum value of 11.8 kcal mol^{-1} is reached at 175° of the initial starting position. With this orientation, the shortest contact, at 3.42 Å, is observed between O(1) and C(3′).

X-ray and Electron Diffraction. Since the actual chain orientation usually deviates slightly from that obtained by packing analysis, the chain is rotated by ±15° from the above orientation, by 5° intervals. At each orientation, the observed and calculated structure factors, for X-ray data and electron diffraction data, are compared after refinement of the scale factor and an overall isotropic temperature factor, B. The values taken by the quantity $R_w = [\sum w\Delta F^2/\sum wF_o^2]^{1/2}$, which measures the agreement between observed and calculated structure factors, are plotted as a function of the chain orientation on Figure

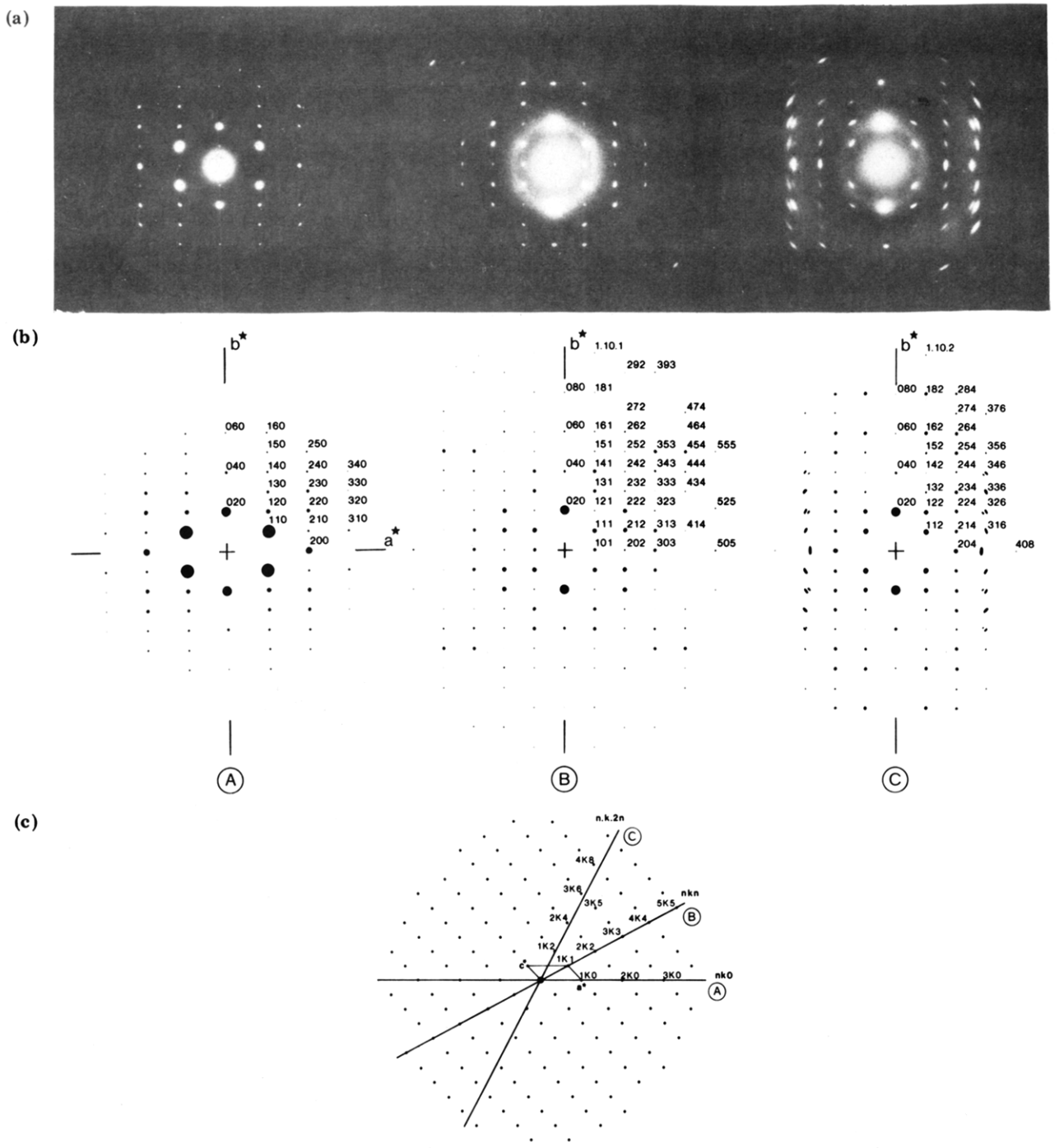

Figure 2. (a) Three electron diffractograms recorded from poly(*t*-CDS) micro single crystals. The tilt axis (vertical) is common to all three patterns. (b) Corresponding indexing of the diffraction spots. (c) View of the reciprocal lattice, perpendicular to the tilt axis. Each electron diffractogram recorded is materialized by its trace on the *h*0*l* section.

7. In the case of the X-ray diffraction data, the minimum value of R_w reached is 0.206 for 29 diffraction spots with $B = 11$ Å^2 and a chain orientation of 172°. In the case of the electron diffraction data, R_w reaches a minimum of 0.199 with $B = 5$ Å^2 when the chain is oriented at 178°. The lists of observed and calculated structure factors corresponding to the above minima are given in Tables V and VI. To reconcile the slightly different chain orientations indicated by the X-ray and electron diffraction data, we have chosen the average orientation of 175° as the most satisfying.

Actually, this is the orientation found by packing analysis and also the one that corresponds to the minimum value of $R = \sum|\Delta F|/\sum F_o$ computed for all observed and unobserved X-ray reflections. The atomic coordinates given in Table IV correspond to this orientation. The X-ray scattering factors were taken from Cromer and Waber[15] for C and O atoms and from Stewart, Davidson, and Simpson[16] for H atoms. The electron scattering factors for C, O, and H atoms were obtained from ref 17.

Discussion

This is one of the very few times that three-dimensional electron diffraction data have been used to confirm the structure of a polymer. Another structure confirmed in a similar manner, that of the cross-polymerized form of poly(1,11-dodecadiyne),[18] was pointed out to us by one of the reviewers. The R_w value of 0.199 is very satisfactory considering that the structure factors were computed in the kinematic approximation. The structure is further

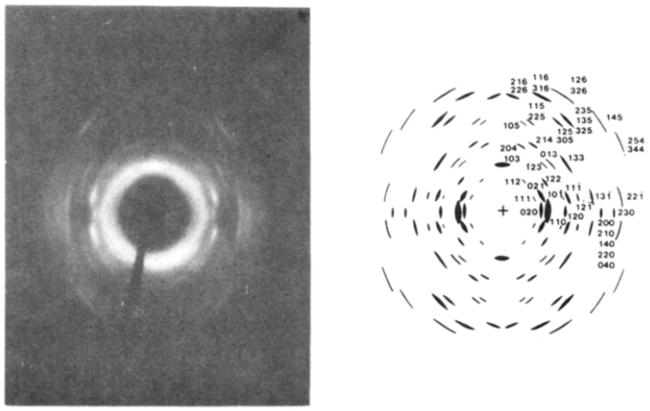

Figure 3. (a) Typical X-ray fiber diagram of poly(*t*-CDS). Most of the weak diffraction spots are not visible. (b) Schematic indexing of the fiber diagram.

Table V
Comparison between the Observed (F_o) and Calculated (F_c) Structure Amplitudes Obtained from the Fiber Diagram

hkl	w^a	F_o	$\|F_c\|$	*hkl*	w^a	F_o	$\|F_c\|$
020	1.00	116	100	114			6
110	1.00	155	179	204	0.75	26	29
120	0.95	58	51	214	0.65	22	17
130			7	124			2
040	0.90	84	15	224			5
200			70	004			12
210			30	014			0
140			18	134			6
220			21	234			14
230	0.65	39	27	024			21
				314			1
011			10	324			4
101			9	034			5
111	1.00	49	41	144			11
021	1.00	106	91	244			3
121			12	334			16
10$\bar{1}$	0.30	24	67	044			1
11$\bar{1}$	0.95	75	79	11$\bar{4}$			3
031			8	154			3
131			3	12$\bar{4}$			3
12$\bar{1}$	0.55	29	18	254	0.45	31	16
211			9	344			19
221			9				
13$\bar{1}$	0.95	64	43	105	0.45	20	17
041			3	115	0.45	30	11
141			16	225			20
231			5	125	0.90	84	66
14$\bar{1}$			17	305			25
21$\bar{1}$			43	315			18
051			12	235	0.95	73	62
22$\bar{1}$	0.55	29	34	135			13
				325			27
112	0.65	14	10	015			1
002			25	025			7
012			19	335			1
122	0.75	23	25	245			5
				145	0.45	29	22
103	0.85	32	39				
113			14	206			27
123	0.65	19	17	216	0.90	38	43
013	0.65	27	26	226			27
213			0	116	0.35	27	10
223			7	316			19
023			11	126	0.45	25	26
133	0.95	49	34	326			24

[a] w is the observational weight attached to each observed measurement.

confirmed when one observes the starred reflections in Table VI. These reflections of the type $3k5$ and $4k7$ were recorded on film C (Figure 2) together with the reflections

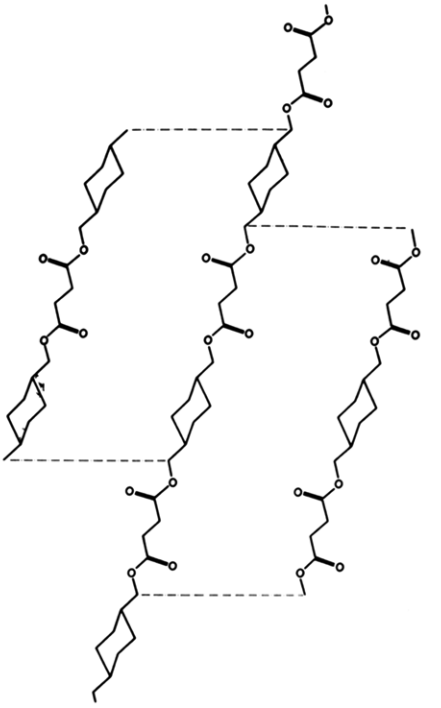

Figure 4. Poly(*t*-CDS) and two of the model compounds that were synthesized. Only the one on the left, 1,4-*trans*-cyclohexanedimethylene 3,3′-bis(methoxycarbonyl)dipropionate, was crystalline.

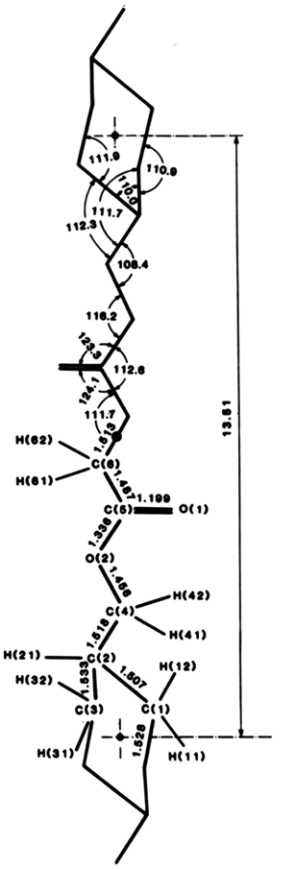

Figure 5. Bond distances and angles, obtained from the model compound, used to build the polymer's repeat unit.

of the $n,k,2n$ zones. Because they were recorded unexpectedly, the intensities of these diffraction spots were not originally included in the refinement. However, as can be seen in Table VI, the agreement between the observed and

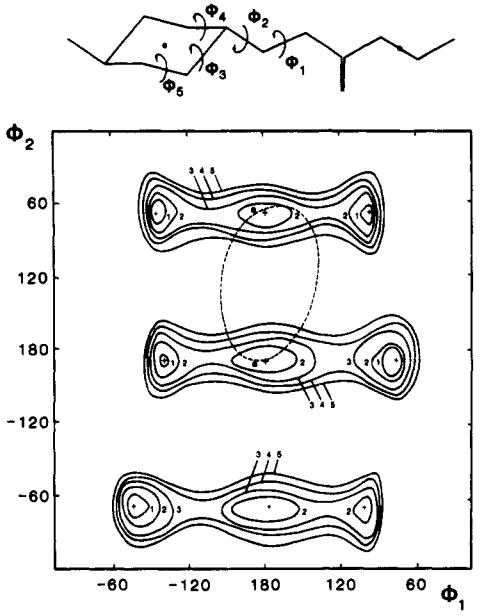

Figure 6. Energy map for poly(*t*-CDS). The energy minima are shown by crosses while the black dots indicate the conformation observed in the model compound. The dotted line corresponds to the fiber repeat of 13.51 Å.

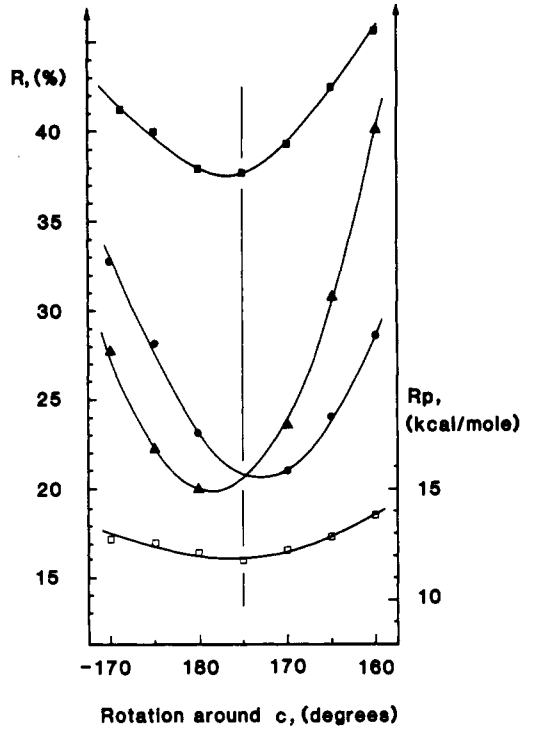

Figure 7. Variation of R_p (□) and the conventional R factors as the chain is rotated as a whole around the c axis from its minimum-energy orientation. The rotation angle is that between the plane formed by the succinate group and the b direction. (▲) R_w for electron diffraction data (observed reflections only); (●) R_w for X-ray data (observed reflections only); (■) R for X-ray data (all the accessible reflections).

calculated structure factors for the starred reflections is as good as for the other reflections. In fact, when they were included in the refinement, R_w remained unchanged. In the accompanying paper[19] we discuss the effect of correcting the electron diffraction data for crystal bending or for the multiple diffraction effects (n-beam dynamical calculation). In both cases, there is a significant improvement of the agreement index, noticeably in the case of the *nk*0 zone. In the case of the *nkn* or *n*,*k*,2*n* zones,

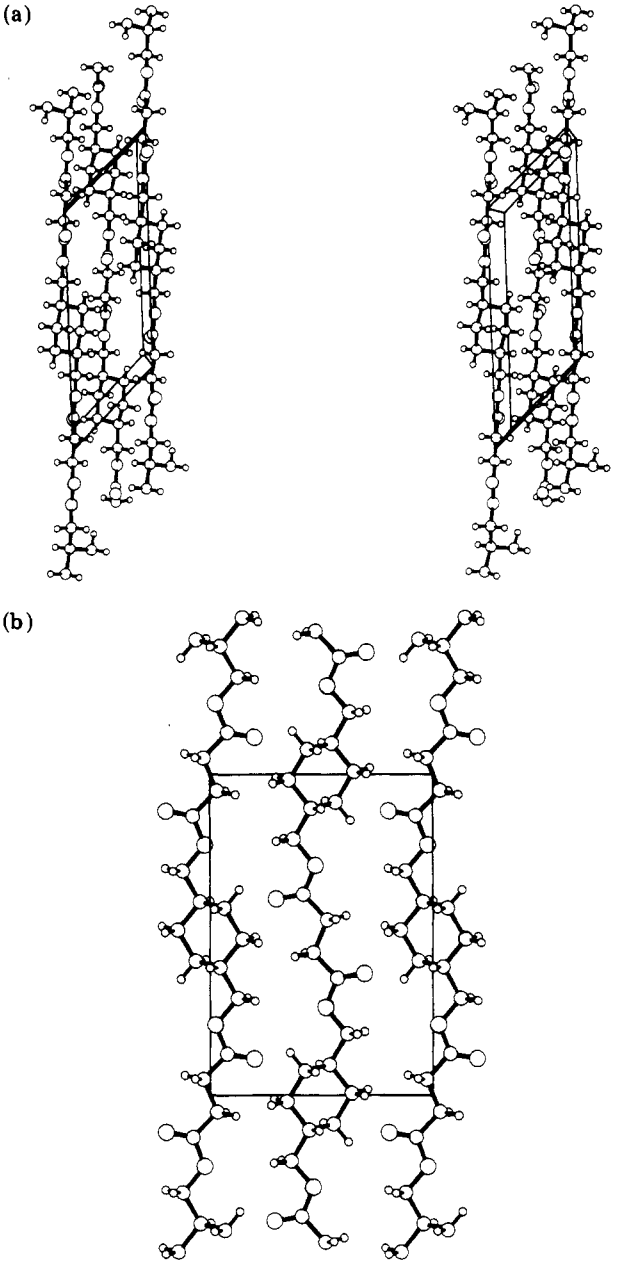

Figure 8. (a) Stereopair showing the chains of poly(*t*-CDS) in their unit cell. (b) Projection of the chains along the *a* axis.

the agreement is not as good, clearly indicating a likely misorientation of the crystal when the diffraction films were recorded.

The R_w value for the X-ray data, although acceptable, is not very low. This could be accounted for by the difficulty we encountered in evaluating the X-ray intensities due to the strong arcing and overlapping of the diffraction spots.

The packing of the polymeric chains of poly(*t*-CDS) is shown by a stereoscopic pair and as a projection on the *bc* plane in Figures 8. The observed conformation for poly(*t*-CDS) in the cyclohexanedimethanol portion is $t_g^t(t\pm gt)_t^{-g}t$ (g, gauche; t, trans), depending which side of the cyclohexane ring is followed. The succinate group is in the trans conformation. The two independent poly(*t*-CDS) chains in the unit cell are out of phase: the succinate group and the 1,4-*trans*-cyclohexanedimethanol moiety of one chain have a half fiber repeat difference with the corresponding groups in the adjacent chains. Although, the polymeric chains of PE4 and PE6 are all in phase,

Table VI
Observed and Calculated Structure Factors of the Electron Diffraction Data of Poly(*t*-CDS)

A, *nk*0 reflections				B, *nkn* reflections				C, *n,k,*2*n* reflections			
hkl	*w*	F_o	$\|F_c\|$	*hkl*	*w*	F_o	$\|F_c\|$	*hkl*	*w*	F_o	$\|F_c\|$
020	1.00	80	77	101	0.90	20	18	112	0.70	25	24
040		20	3	111		25	22	122		17	14
060		10	6	121		3	2	132		9	4
080		5	4	131		14	3	142		5	1
110		140	142	141		14	13	152		7	5
120		32	34	151		7	2	162		10	8
130		22	3	161		7	4	172			4
140		16	13	171			2	182		7	6
150		7	6	181		5	4	192			2
160		4	1	191			0	1,10,2		4	3
200		65	61	1,10,1		5	3	204		25	22
210		19	14	202		12	3	214		13	15
220		22	20	212		19	21	224		14	17
230		21	28	222		16	16	234		10	16
240		4	2	232		7	2	244		5	5
250		5	2	242		9	3	254		17	19
310		14	15	252		3	2	264		10	15
320		11	10	262		9	4	274		9	7
330		6	7	272		3	1	284		10	10
340		6	10	282			2	305*	0.40	39	32
				292		9	6	315*		10	9
				303		12	1	325*		19	24
				313		11	11	335*			1
				323		4	3	345*		12	17
				333		4	4	355*		7	6
				343		5	4	316	0.70	14	20
				353		7	6	326		19	30
				363			2	336		27	27
				373			1	346		5	5
				383			2	356		12	10
				393		9	7	366			3
				404			1	376		7	6
				414		7	7	417*	0.40	4	7
				424			8	427*		7	8
				434		8	6	437*			3
				444		9	3	447*			2
				454		16	15	457*		7	8
				464		5	4	467*		6	7
				474		9	5	408	0.70	10	10
				505		12	9				
				515			1				
				525		5	2				
				535			4				
				545			0				
				555		5	6				

Turner-Jones and Bunn[4] reported the existence of a second crystalline form for PE4 where the adjacent chains are out of phase.

The structural similarities noted between the chains of terephthalate polyesters such as poly(ethylene terephthalate) and poly(*t*-CDT)[5] are no longer present when one compares the analogous pair of succinate polyesters, PE2[3] and poly(*t*-CDS). The observed density and the space group of both PE2 and poly(*t*-CDS) require that these polymeric chains possess some kind of symmetry elements of their respective unit cells. However, the symmetry imposed on the PE2 chain is that of a twofold axis of rotation perpendicular to the fiber axis, while the poly(*t*-CDS) chain must pass through some of the centers of symmetry of its unit cell.

The crystal structure of poly(*t*-CDS) is the same whether the material is in the fiber form (X-ray data) or as a micro single crystal (electron diffraction data). The same situation has already been reported for poly(trimethylene terephthalate).[20] Figure 1c shows the correlation between single crystals and the packing of the chains in projection. The sides of the crystal correspond to (110) planes. These crystal planes are parallel to the direction of highest atomic densities (Figure 1c). Indeed, the 110 reflection is found to be the strongest among all the observed reflections.

Acknowledgment. We thank the Natural Sciences and Engineering Research Council of Canada for its financial support through a grant in aid of research (Grant No. A5968) and for the scholarship granted to B.R., F.B. thanks the authorities of the Université de Montréal for according a sabbatical leave of absence and acknowledges the hospitality of the staff of the Centre de Recherche sur les Macromolécules Végétales (CERMAV), Grenoble, France, for their patience and help in the taking of the electron diffraction patterns of poly(*t*-CDS).

Registry No. (*trans*-1,4-Cyclohexanedimethanol)·(succinic acid) (copolymer), 81381-36-4; poly(1,4-*trans*-cyclohexanediyldimethylene succinate), (SRU), 81381-32-0.

References and Notes

(1) Fuller, C. S.; Erickson, C. L. *J. Am. Chem. Soc.* **1937**, *59*, 344.
(2) Fuller, C. S.; Frosch, C. J.; Pape, N. R. *J. Am. Chem. Soc.* **1942**, *64*, 154.
(3) Ueda, A. S.; Chatani, Y.; Tadokoro, H. *Polym. J.* **1971**, *2*, 387.
(4) Turner-Jones, A.; Bunn, C. W. *Acta Crystallogr.* **1962**, *15*, 105.
(5) Rémillard, B.; Brisse, F. *Polymer* **1982**, *23*, 1960.
(6) Collins, E. A.; Bares, J.; Billmeyer, F. W. "Experimental in Polymer Science"; Wiley-Interscience: New York, 1973; pp 131–135.

(7) Iwakura, Y.; Taneda, Y.; Ushida, S. *J. Appl. Polym. Sci.* **1961**, *5*, 108.
(8) Brisse, F.; Rémillard, B. *Acta Crystallogr., Sect. B* **1982**, *B38*, 825.
(9) Scott, R. A.; Scheraga, H. A. *J. Chem. Phys.* **1966**, *44*, 3054.
(10) Scott, R. A.; Scheraga, H. A. *J. Chem. Phys.* **1966**, *45*, 2091.
(11) Brant, D. A.; Miller, W. G.; Flory, P. J. *J. Mol. Biol.* **1967**, *23*, 47.
(12) Smyth, C. P. In "Dielectric Behaviour and Structure"; McGraw-Hill: New York, 1955.
(13) Wyckoff, R. W. G. In "Crystal Structures"; Wiley: New York, 1965; Vol. I.
(14) William, D. E. *Acta Crystallogr., Sect. A* **1969**, *A25*, 464.
(15) Cromer, D. T.; Waber, J. T. *Acta Crystallogr.* **1965**, *18*, 104.
(16) Stewart, R. I.; Davidson, E. R.; Simpson, W. T. *J. Chem. Phys.* **1965**, *42*, 3175.
(17) "International Tables for X-Ray Crystallography"; Kynoch Press: Birmingham, 1974; Vol. IV.
(18) Thakur, M.; Lando, J. B. *Macromolecules* **1983**, *16*, 143.
(19) Moss, B.; Brisse, F. *Macromolecules*, see accompanying Note in this issue.
(20) Poulin-Dandurand, S.; Pérez, S.; Revol, J.-F.; Brisse, F. *Polymer* **1979**, *20*, 419.

Block Copolymers near the Microphase Separation Transition. 1. Preparation and Physical Characterization of a Model System

Frank S. Bates,* Harvey E. Bair, and Mark A. Hartney

AT&T Bell Laboratories, Murray Hill, New Jersey 07974. *Received November 22, 1983*

ABSTRACT: A model set of 1,4-polybutadiene–1,2-polybutadiene diblock copolymers has been prepared and molecularly characterized. Physical characterization by differential scanning calorimetry (DSC) and qualitative identification of the flow behavior (liquid- vs. solid-like) over a period of several days have established the critical degree of polymerization for this system as $N_c = 1.20\ (\pm 0.14) \times 10^3$. Below the microphase separation transition the polymers exhibit a single broad glass transition, as measured by DSC, which has been attributed to local segment density fluctuations. This effect was found to be dependent on the degree of polymerization, as predicted from theory.

Introduction

The general phenomenon of polymer–polymer immiscibility is a natural consequence of the size of macromolecules, which results in a vanishingly small entropy of mixing relative to monomers. Homogeneous polymer–polymer systems are therefore quite rare, which severely hampers attempts to alloy polymers in the manner in which metals and ceramics are formulated. Nevertheless, it has been demonstrated that the blending of polymers can produce synergistic effects (e.g., polystyrene and poly(phenylene oxide)[1]) and considerable energy has been expended over the past several decades in an effort to elucidate the underlying physics which govern such systems.

Flory[2] provided one of the first representations for the free energy of mixing in homopolymer blends based on a liquid lattice model in which the energy of interaction of different chemical species per site is defined as

$$F_{int} = kT\chi\Phi(1 - \Phi) \tag{1}$$

where k is the Boltzmann constant, T is the temperature, and Φ is the volume fraction of one component. χ is the dimensionless Flory interaction parameter, which persists today as the most common basis for describing the interaction energy between polymer segments (and solvents). In polymer blends governed by van der Waals interactions ($\chi \geq 0$), increasing χ above a critical value produces phase separation, while at very small (or negative) χ, entropy effects dominate, resulting in miscibility. In general, for $\chi \geq 0$, χ is assumed to be constant for a particular pair of polymers, and the product of χ and the degree of polymerization N is the parameter which determines miscibility for a given Φ. The critical point, defined as $\partial^3(F/kT)/\partial\Phi^3 = 0$, occurs at

$$\chi_c = (N_B^{1/2} + N_A^{1/2})^2/2N_AN_B \tag{2}$$

where N_A and N_B are the degrees of polymerization of each component. For the symmetrical case $N_A = N_B = N/2$, for which $(N\chi)_c = 4$.

Recently, Leibler[3] has derived a theory of microphase separation in block copolymers exhibiting an upper critical solution temperature (UCST). The criteria for stability and equilibrium are too cumbersome to be reproduced here and so only the results are shown in Figure 1. Such systems contain a single critical point at $\Phi = 0.5$ which is predicted to scale as

$$(N\chi)_c = 10.5 \tag{3}$$

where $N = N_A + N_B$.

The phase behavior of polymer blends is best studied by means of scattering experiments (e.g., light X-ray, or neutron scattering). The scattering power, $S(q)$, of a homogeneous blend of homopolymers increases and finally diverges at $q \to 0$ as the spinodal curve is approached from the homogeneous melt,[4] where q ($=4\pi\lambda^{-1} \sin(\theta/2)$) is the magnitude of the scattering wave vector. Such scattering results from the development of local segment density fluctuations. In practice, little data exist concerning such critical fluctuations in polymers since it is difficult to distinguish between the equilibrium and spinodal limits in a homopolymer blend and because such long times are required to attain equilibrium.

Block copolymers are considerably more attractive for studying polymer–polymer interactions in the homogeneous melt state and near the phase transition boundaries. The block nature of these materials limits the range of density fluctuations to molecular dimensions, thereby reducing the time required to attain equilibrium. In homopolymer blends the range of fluctuations is unbounded. Also, the elevated critical molecular weight provides a significant increase in N over which a given system should remain homogeneous. As illustrated in Figure 1, the equilibrium and stability boundaries are predicted to be almost commensurate. This provides an opportunity to measure equilibrium properties over almost the entire

0024-9297/84/2217-1987$01.50/0